Journal of Molecular Catalysis A: Chemical 310 (2009) 42–50

Contents lists available at ScienceDirect

Journal of Molecular Catalysis A: Chemical

journal homepage: www.elsevier.com/locate/molcata

Immobilization of anionic iron(III) porphyrins into ordered macroporous layered double hydroxides and investigation of catalytic activity in oxidation reactions

Matilte Halma[a], Kelly Aparecida Dias de Freitas Castro[a], Vanessa Prévot[b], Claude Forano[b], Fernando Wypych[a], Shirley Nakagaki[a,*]

[a] Laboratory of Bioinorganic Chemistry and Catalysis, Department of Chemistry, Federal University of Paraná, P.O. Box 19081, Zip Code 81531-980, Curitiba, PR, Brazil
[b] Laboratoire des Matériaux Inorganiques, UMR CNRS 6002, Université Blaise Pascal, 63177 Aubière Cedex, France

ARTICLE INFO

Article history:
Received 26 February 2009
Received in revised form 18 May 2009
Accepted 22 May 2009
Available online 30 May 2009

Keywords:
Porphyrin
Cytochrome P-450 model
Catalysis
Oxidation
Macroporous layered double hydroxides

ABSTRACT

The first generation anionic iron(III) porphyrin [Fe(TSPP)] and the second generation anionic complexes [Fe(TDFSPP)], [Fe(TCFSPP)], and [Fe(TDCSPP)] were immobilized into three-dimensionally macroporous layered double hydroxide (3DM-LDH), using the direct reconstruction of 3DM-LDH from macroporous mixed oxides MOX or the anionic exchange on DDS intercalated 3DM-LDH. The macroporous layered double hydroxides were obtained at the surface of nanometric polystyrene spheres, which were synthesized by an inverse opal method. Polystyrene was removed after calcination in oxidizing atmosphere, nanostructured mixed oxides (3DM-MOX) were obtained, which after reconstruction give origin to macroporous layered double hydroxide (3DM-LDH). Following metalloporphyrin immobilization, the resulting materials were characterized by powder X-ray diffraction (PXRD), scanning electron microscopy (SEM), UV–vis (glycerin mull) spectroscopy, attenuated total reflectance Fourier transform infrared spectroscopy (ATR/FTIR), and electron paramagnetic resonance (EPR). Results revealed that the complexes are either immobilized at the surface of the macroporous layered double hydroxide or intercalated between the layers, displacing some dodecylsufate anions. The obtained materials were investigated as catalysts for oxidation reactions, to find out whether they function as cytochrome P-450 models.

1. Introduction

Metalloporphyrin-based oxidation catalysts capable of mimicking the enzymatic reactions performed by the cytochrome P-450 family have been extensively reported over the last three decades. One explanation for the extraordinary activity in this research area is that model systems based on iron and manganese porphyrins present similar efficiency and selectivity to those achieved with biological systems, especially in the case of the catalytic conversion of cyclic alkanes to alcohol and of alkenes to epoxide, in mild conditions [1–9]. The pioneering work in this research area was carried out by Groves in the 1970s, when the use of synthetic iron porphyrins (FePs) as cytochrome P-450 model was introduced [10,11]. Because the metalloporphyrin skeleton was oxidatively degraded under the oxidation reaction conditions, many efforts have been made toward the synthesis and evaluation of a large variety of porphyrin analogues in an attempt to improve their catalytic activity and robustness [12–15]. In this sense, second generation metalloporphyrins were synthesized by introduction of electron-withdrawing groups on the phenyl substituents of the porphyrin ring [12,16–19]. These metalloporphyrins were shown to be more resistant toward oxidative degradation than simpler metalloporphyrins like the first-generation iron(III) tetraphenylporphyrin [Fe(TPP)] employed by Groves [10,12,20–23].

Another method for the preparation of more robust and efficient catalysts for oxidation reactions under biomimetic conditions consists in the immobilization of metalloporphyrins in inorganic and organic solid supports. One expected advantage of this procedure is the possible reuse of the heterogenized catalysts. Reusable and recyclable oxidation catalysts based on efficient and selective metalloporphyrins open perspectives for the future technological applications of these robust molecules, which is particularly attractive from an economic and environmental point of view [24–36]. Furthermore, depending on the support, there are several other advantages, like promotion of a special environment for substrate approach to the catalytic active species, which can favor more selective reactions [24,29,37–40]. In this context, many different inorganic and organic solids have been investigated as supports for metalloporphyrin immobilization. Inorganic solids, like silica, alumina, zeolite, clay minerals, and a large number of layered synthetic compounds, have been successfully employed for immobilization of different metalloporphyrin generations, as well as organic polymers, such as polystyrenes and synthetic resins. We have recently concentrated our efforts on the use of layered double hydroxides

* Corresponding author. Tel.: +55 41 3361 3180; fax: +55 41 3361 3186.
E-mail address: shirley@quimica.ufpr.br (S. Nakagaki).

1381-1169/$ – see front matter © 2009 Elsevier B.V. All rights reserved.
doi:10.1016/j.molcata.2009.05.017

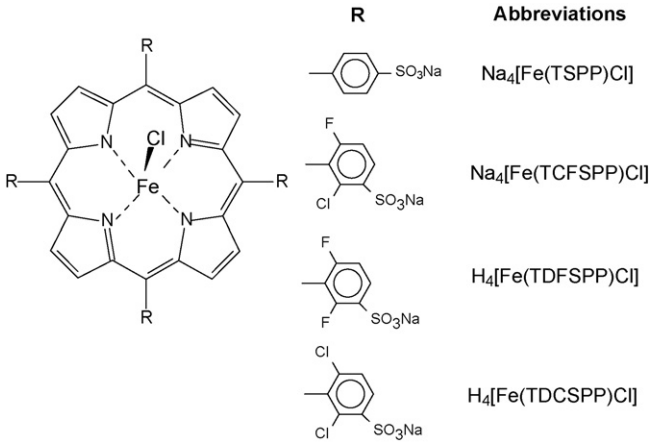

Fig. 1. Schematic representation of the iron(III) porphyrins employed in this work.

(LDHs) as inorganic supports for metalloporphyrin immobilization [24–28,31,38–42].

The LDH support is advantageous because it is catalytically inert and easy to obtain, it is very resistant to the biomimetic reaction conditions employed in the oxidation of organic substrates in the presence of metalloporphyrins, it can be used in a wide range of solvents, and it is easily recovered from the reaction medium. LDHs typically consist of layers of metal cations (M^{II} and M^{III}) of similar ionic radii coordinated by six hydroxyl groups, forming $M^{II}/M^{III}(OH)_6$ octahedral. These octahedrals share their edges, thus leading to two-dimensional layers. These layers are stacked along the basal directions and separated by hydrated charge-balancing anions, and they are stabilized by electrostatic forces and hydrogen bonding [29,43–46]. Because of their layered structure and anion exchange ability, LDHs have recently been intensively investigated as hosts for incorporation of organic moieties by several methods [46–51]. The original synthetic pathway for the preparation of nanostructured LDH materials through control of the textural properties in terms of morphology, particle size, specific area, and pore structure has been recently developed. The synthesis of three-dimensionally ordered macroporous MgAl–LDHs has been performed using a colloidal crystal templating method [52–54].

In this work, we report the immobilization of the anionic iron(III) porphyrins (FePs) [Fe(TSPP)], [Fe(TDFSPP)], [Fe(TCFSPP)], and [Fe(TDCSPP)] (Fig. 1) into macroporous LDH (3DM-LDH) as well as the use of these immobilized complexes as cytochrome P-450 biomimetic model catalysts for cyclooctene, cyclohexane, and heptane oxidation.

2. Experimental

2.1. Materials

All solvents and reagents were commercial grade (Aldrich, Merck, Fluka), unless otherwise stated. Authentic samples of the alcohols, ketones, and epoxides that could be produced in the oxidation reactions were purchased at their highest commercial purity grade (Aldrich) and used as received. The substrates cyclooctene, cyclohexane, and heptane were stored at 5 °C and purged with argon prior to use. Cyclooctene was also pre-purified by column chromatography using neutral alumina. After the experiments, all reagents were discarded in an appropriate container for later treatment and reuse when possible, or for final disposal.

2.1.1. Porphyrins

Reagent grade free-base porphyrin [H_2(TSPP)]; [5,10,15,20-tetrakis(4-sulfonatophenyl)porphyrin] was purchased from Aldrich and used without prior purification. The second generation free-base porphyrins [H_2(TDFSPP)]-[5,10,15,20-tetrakis(2,6-difluoro-3-sulfonatophenyl)porphyrin]; [H_2(TCFSPP)]-[5,10,15,20-tetrakis (2-chloro-6-fluoro-3-sulfonatophenyl) porphyrin]; and [H_2(TDCSPP)]-[5,10,15,20-tetrakis(2,6-dichloro-3-sulfonatophenyl)porphyrin] were synthesized and purified by previously described methods. In this work, the anionic tetra charges have been omitted for all the free-base porphyrins for simplification (Fig. 1) [14,30,55].

2.1.2. Iron(III) porphyrins (FePs)

Iron(III) porphyrins were obtained by iron(III) insertion into the free-base porphyrin ligands using ferrous chloride tetrahydrate in dimethylformamide, as described by Adler and Longo [56,57]. Purification of the FePs was performed by column chromatography on Sephadex, using deionized water as eluent. The products were characterized by UV–vis and EPR spectroscopies. Data were consistent with those of the compound expected after the iron insertion reaction. UV/vis data: [Fe(TSPP)Cl] (deionized water) 394 nm ($\varepsilon = 2.4 \times 10^4$ L mol^{-1} cm^{-1}), [Fe(TDFSPP)Cl] (deionized water) 394 nm ($\varepsilon = 3.7 \times 10^4$ L mol^{-1} cm^{-1}), [Fe(TCFSPP)Cl] (deionized water) 390 nm ($\varepsilon = 8.2 \times 10^4$ L mol^{-1} cm^{-1}), and [Fe(TDCSPP)Cl] (deionized water) 390 nm ($\varepsilon = 1.7 \times 10^4$ L mol^{-1} cm^{-1}). The anionic tetra charges have been omitted for all the FePs for simplification.

2.1.3. Iodosylbenzene (PhIO)

PhIO was obtained through hydrolysis of iodosylbenzene diacetate, following previously described methods [58,59]. Purity was periodically checked by iodometric assay.

2.2. Preparation of macro-LDH

The 3DM-LDH was prepared using the inverse opal method as previously reported [54]. Polystyrene spheres (600 ± 20 nm), prepared by emulsion free polymerization were disposed in closed-packed colloidal arrays by centrifugation at 1200 rpm for 12 h. After removal of water, the resulting solid was air-dried. Then, it was permeated with a 1 mol L^{-1} solution (water:ethanol 1:1 mixture) of magnesium and aluminum chloride salts with ratio Mg^{2+}/Al^{3+} of 2 during 48 h, the excess of solution being removed after 48 h by a slight filtration. After drying, the sample was immersed into a 2 mol L^{-1} sodium hydroxide aqueous solution to achieve the templated LDH precipitation. The excess of solution was removed and the sample was washed several times with deionized water and dried. The polystyrene was removed from the composite by calcination at 420 °C for 12 h in a tubular oven, with flux of air [60]. The Mg–Al nanostructured mixed oxides obtained (noted hereafter 3DM-MOX) were used for the immobilization of iron(III)porphyrins and dodecylsufate (DDS) anions. The chemical analysis confirm the expected Mg^{2+}/Al^{3+} molar ratio corresponding to a formula $Mg_2Al(OH)_6X_{1/q}\cdot nH_2O$ (with X^{q-} = DDS^-, Fe(III)porphyrin^{4-}).

2.3. Immobilization of [Fe(TSPP)], [Fe(TDFSPP)], [Fe(TCFSPP)] and [Fe(TDCSPP)] into macroporous LDH

The different iron(III)porphyrins were immobilized into macroporous LDH by regeneration of the calcined sample (3DM-MOX) in deionized water containing the iron(III) porphyrin leading to 3DM-FeP-LDH and by anionic exchange on 3DM-LDH intercalated dodecylsufate anions, resulting in 3DM-FeP-DDS-LDH.

2.3.1. Reconstruction (3DM-MOX) method

A [Fe(TSPP)] aqueous solution was prepared in deionized water (3.33×10^{-5} mol L^{-1}) and purged with nitrogen for 2 h. Then, the calcined solid 3DM-MOX (1.83×10^{-2} g) was added to the FeP, and the mixture was left at room temperature, without stirring,

Table 1
Immobilization of FePs on 3DM-LDH.

Reconstruction (3DM-MOX) method			
Solid obtained	[FeP] (mol L^{-1})[a]	MOX (g)[b]	FeP/LDH (mol/g)[c]
[Fe(TSPP)]-LDH	3.3×10^{-5}	1.8×10^{-2}	8.9×10^{-4}
[Fe(TDFSPP)]-LDH	4.6×10^{-4}	2.0×10^{-2}	9.3×10^{-4}
[Fe(TCFSPP)]-LDH	4.2×10^{-4}	1.8×10^{-2}	6.4×10^{-4}
[Fe(TDCSPP)]-LDH	3.9×10^{-4}	3.0×10^{-2}	2.9×10^{-4}
Anionic exchange method			
Solid	[FeP] (mol L^{-1})[a]	LDH-DDS (g)[b]	FeP/LDH (mol/g)[c]
[Fe(TDFSPP)]-LDH-DDS	2.8×10^{-3}	2.7×10^{-2}	1.2×10^{-3}
[Fe(TCFSPP)]-LDH-DDS	7.5×10^{-4}	3.2×10^{-2}	2.7×10^{-4}
[Fe(TDCSPP)]-LDH-DDS	4.4×10^{-3}	1.9×10^{-2}	3.4×10^{-3}

[a] Iron porphyrin concentration used in the immobilization process.
[b] Matrix mass.
[c] Iron porphyrin loading obtained for the prepared solids (mol of iron porphyrin per gram of solid).

under nitrogen atmosphere for 24 h. The second generation FePs [Fe(TDFSPP)], [Fe(TCFSPP)], and [Fe(TDCSPP)] were immobilized by the same method (Table 1).

2.3.2. Anionic exchange method

The LDH-DDS solid was prepared according to the reconstruction (3DM-MOX) method described above, using aqueous solution of two fold excess NaDDS over Al^{3+} content [54]. Then, a FeP anion was dissolved in an H_2O/EtOH (1:1, v/v) solvent mixture (2.77×10^{-3} mol L^{-1}) and maintained under nitrogen atmosphere for 30 min. The LDH-DDS solid was added to the FeP solution, and the mixture was left at room temperature under magnetic stirring and nitrogen atmosphere for 24 h (Table 1).

After the immobilization reactions, [Fe(TSPP)]-LDH, [Fe(TDFSPP)]-LDH, [Fe(TCFSPP)]-LDH, [Fe(TDCSPP)]-LDH, [Fe(TDFSPP)]-LDH-DDS, [Fe(TCFSPP)]-LDH-DDS, and [Fe(TDCSPP)]-LDH-DDS were washed with deionized water and recovered by centrifugation. The combined washing solutions were stored and analyzed by UV–vis spectroscopy, to quantify the amount of exchanged Fe(III) porphyrins. The obtained brown solids were air-dried, and their FeP/solid loadings are presented in Table 1.

2.4. Oxidation of cyclooctene, cyclohexane, and heptane by PhIO catalyzed by anionic FePs in homogeneous medium or immobilized into macro-LDH

The oxidation reactions were carried out in a thermostatic glass reactor (2 mL) equipped with a magnetic stirrer, placed inside a dark chamber [35,41]. In the case of the FeP/3DM-LDH solids (heterogeneous catalysis), the solid catalyst and iodosylbenzene (in a FeP/PhIO molar ratio 1:10) were suspended in dichloromethane/acetonitrile 1:1 (v/v) mixture (0.350 mL) and degassed with argon for 15 min. The substrate (cyclooctene, cyclohexane, or heptane) was then added to the glass reactor at a FeP/substrate molar ratio of 1:1000, and the oxidation reaction was performed for 1 h under magnetic stirring. Sodium sulfite was added in the end, to eliminate any excess iodosylbenzene and to quench the reaction. The reaction products were separated from the solid catalyst (heterogeneous catalysis) by exhaustive washing and centrifugation of the FeP-macro-LDH catalyst with a dichloromethane/acetonitrile 1:1 (v/v) mixture. The combined washing solutions were analyzed by capillary gas chromatography. The products were identified by comparison of their retention times with those of authentic samples. Product yields were determined by means of the internal standard method. Control reactions were carried out with the chlorine-intercalated macro-LDH containing no FeP, and with a solution blank set up without any solid. A similar procedure was adopted when FePs were employed as homogeneous catalyst.

2.5. Characterization techniques

Particle size was measured with a Malvern Zetasizer (Nano ZS) from dilute samples of PS sphere suspensions. SEM characteristics of the samples were imaged by either a JEOL 5190 microscope operated at 15 keV or a JEOL JSM-6360LV operating at 15 keV. X-ray powder diffraction patterns (XRPD) were recorded in the reflection mode using a Shimadzu XRD-6000 diffractometer operating at 40 kV and 40 mA, using CuKα radiation (λ = 1.5418 Å) and a dwell time of 1° min^{-1}. UV–vis spectra (UV–vis) were performed on the NICOLET evolution 500-Diode Array spectrophotometer, using solid samples dispersed in glycerol mulls placed between two quartz plates. Electron paramagnetic resonance (EPR) spectra of the FeP-macro-LDH systems in the solid state were obtained on a Bruker ESP 300E spectrometer operating at the X-band (approximately 9.5 GHz), at 77 K, using liquid N_2. Products from the catalytic oxidation reactions were identified using a Shimadzu CG-14B gas chromatograph equipped with a flame ionization detector and a DB-WAX capillary column (J & W Scientific).

3. Results and discussion

3.1. Preparation and characterization of the FeP/3DM-LDH catalysts

In this work, we prepared three-dimensionally ordered macroporous LDH (3DM-LDH) materials for the immobilization of second generation of Fe(III) porphyrin catalysts with improved catalytic efficiency due to textural control. The 'inverse opals method' was performed using polystyrene (PS) opals as template. Interestingly, PS spheres can be produced as monodispersed microspheres under the surfactant-free emulsion polymerization. Moreover, PS spheres can be easily removed by a moderate calcination [54]. The nanotextured hydrotalcite solid $Mg_2Al(OH)_6(CO_3)_{0.5}$ described in this study is obtained by co-precipitation of divalent and trivalent metallic cations, taking place inside the voids of the PS colloid crystal after successive infiltrations.

The measurements of zeta potential and granulometry confirm that emulsifier-free emulsion polymerization produces very monodisperse PS spheres (polydispersity index lower than 0.1) of 600 ± 20 nm particle size, and that these beads are negatively charged with a zeta potential of −47 mV. Crystallization of the opal is controlled by repulsive electrostatic forces between spheres.

The SEM micrographs (Fig. 2) reveal that an ordered array of monodispersed beads is obtained (Fig. 2A), thus confirming that the order of the PS crystal template is preserved during the different processes of infiltration, precipitation and drying. Note that from SEM images, LDH-type particles are not distinguishable, which means that the inorganic material is filling the template voids, thus forming a wall-type structure around the PS beads (Fig. 2B).

The solids obtained from regeneration of the calcined sample (3DM-OX) in porphyrin solutions ([Fe(TSPP)]-LDH, [Fe(TDFSPP)]-LDH, and [Fe(TCFSPP)]-LDH, Fig. 3b–d, respectively) and the solids obtained by ionic exchange with DDS anions ([Fe(TDCSPP)]-LDH-DDS, [Fe(TCFSPP)]-LDH-DDS, and [Fe(TDFSPP)]-LDH-DDS, Fig. 3e–g, respectively) were submitted to powder X-ray diffraction analysis (PXRD). The X-ray diffraction patterns obtained for the PS spheres (Fig. 3a) are characterized by two large humps, a small one around 10° and an intense one in the region of 15–30° (in 2θ). Such humps correspond to the organization of semi-crystalline state in the polystyrene [54,60].

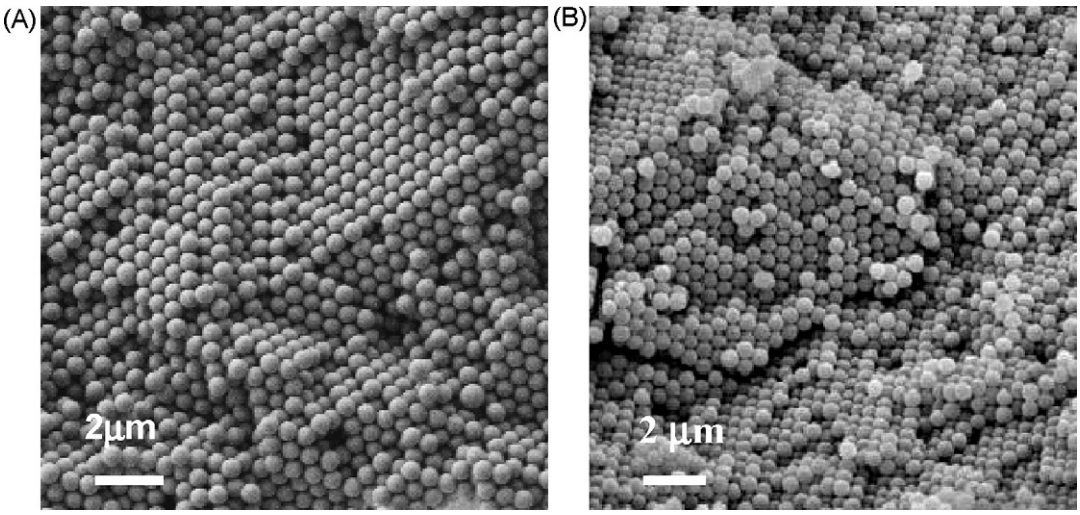

Fig. 2. SEM images of (A) PS crystal and (B) PS–LDH composite.

The nanostructured Mg/Al mixed oxides (3DM-OX) obtained by LDH ($Mg_2Al(OH)_6(CO_3)_{0.5}$)/PS calcination were successively reconstructed in the presence of a FeP or DDS anion containing solution, as confirmed by the PXRD patterns (Fig. 3b–g). The X-ray diffraction patterns display the typical pattern of layered compounds, with (0 0 l) and (*h k l*) reflections [43,44,61]. The observed basal distance of 7.8 Å is characteristic of carbonate anion intercalation in LDH [35,61] (Fig. 3b–d). For the phases obtained by anionic exchange on LDH-DDS (Fig. 3e–g), a basal distance of 25.5 Å is observed, in agreement with values found in the literature for DDS anions intercalated between the LDH layers [42,62,63]. On the point of view of structural consideration, intercalation of FeP by direct regeneration from 3DM-MOX method does not occurred, only LDH-CO_3 phases are formed. However, chemical analysis evidences the presence of FeP on the solids in relative quantitative amounts (respectively 90.6%, 62.4% and 28.3% of the anionic exchange capacity for [Fe(TDFSPP)]-LDH, [Fe(TCFSPP)]-LDH and [Fe(TDCSPP)]-LDH) (Table 1). Obviously, Fe(III) porphyrin anions are chemisorbed at the surface of meso- and macropores of the 3DM-LDH materials. For the FeP exchanged on 3DM-DDS-LDH, anionic porphyrins may be either intercalated in between the LDH layers or adsorbed at the surface of the platelets. Because of the presence of DDS anionic pillars, the final products retained the highest basal spacing characteristic of DDS containing LDH phases (d = 25.5 Å). With dimensions lower than DDS anions FeP molecules (16.0 Å × 15.8 Å × 4.3 Å for Fe-TSPP for example) cannot imposed the interlayer spacing. Indeed, pure LDH compounds intercalated by Fe(III) porphyrins display lower basal spacing between 20 and 23 Å as we previously reported [36,41]. Interestingly DDS bilayers and FeP species exhibit a high chemical and structural compatibility leading to possible co-immobilization. Chemical analysis obtained for these phases reveals higher amounts of immobilized FeP catalysts (Table 1).

The inorganic materials are observed by SEM after the subsequent treatments of calcination of the template (Fig. 4A) and regeneration in the different anionic solutions (Fig. 4B–D). We can note that after thermal treatment, the mixed oxides obtained display as expected a well-ordered macroporous structure, evidencing that during the PS removal, an inorganic replica of the starting array is obtained (Fig. 4A). The macroporous structure is also maintained during the LDH structure regeneration in DDS aqueous solution, leading to a macroporous DDS intercalated LDH (Fig. 4B). During the reconstruction process, the thickness of the walls is increased and the level of 3D order is decreased due to the large organic anion intercalation into the LDH lamellar structure. In the case of direct regeneration of 3DM-FeP-LDH, similar nanostructured phases are obtained with the maintenance of ordered arrays of macroporous lattice while by the anionic exchange method the macroporous network is slightly disturbed.

The presence of FeP in the macro-LDH matrix is confirmed by UV–vis spectra of the solids in glycerin mull (Fig. 5). There are two sets of absorption bands in the UV–vis spectra of porphyrins. The Soret band is characterized by a large absorption coefficient and lies in the 400–450 nm range. A second set of weaker bands (the Q bands) occurs between 450 and 700 nm [51]. The measurements suggest that no demetallation, characterized by a blue-shift

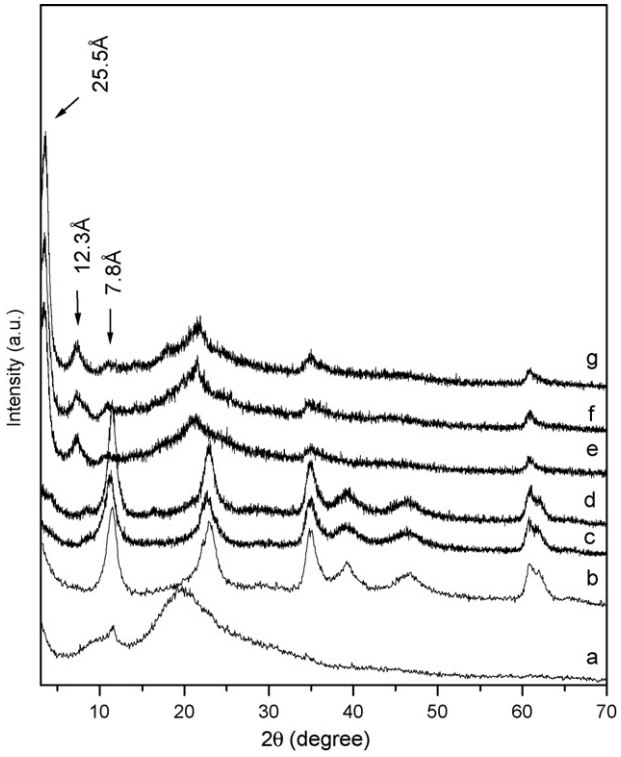

Fig. 3. PXRD patterns for (a) PS2, (b) [Fe(TSPP)]-LDH, (c) [Fe(TDFSPP)]-LDH, (d) Fe[(TCFSPP)]-LDH, (e) [Fe(TDCSPP)]-LDH-DDS, (f) [Fe(TCFSPP)]-LDH-DDS, and (g) [Fe(TDFSPP)]-LDH-DDS.

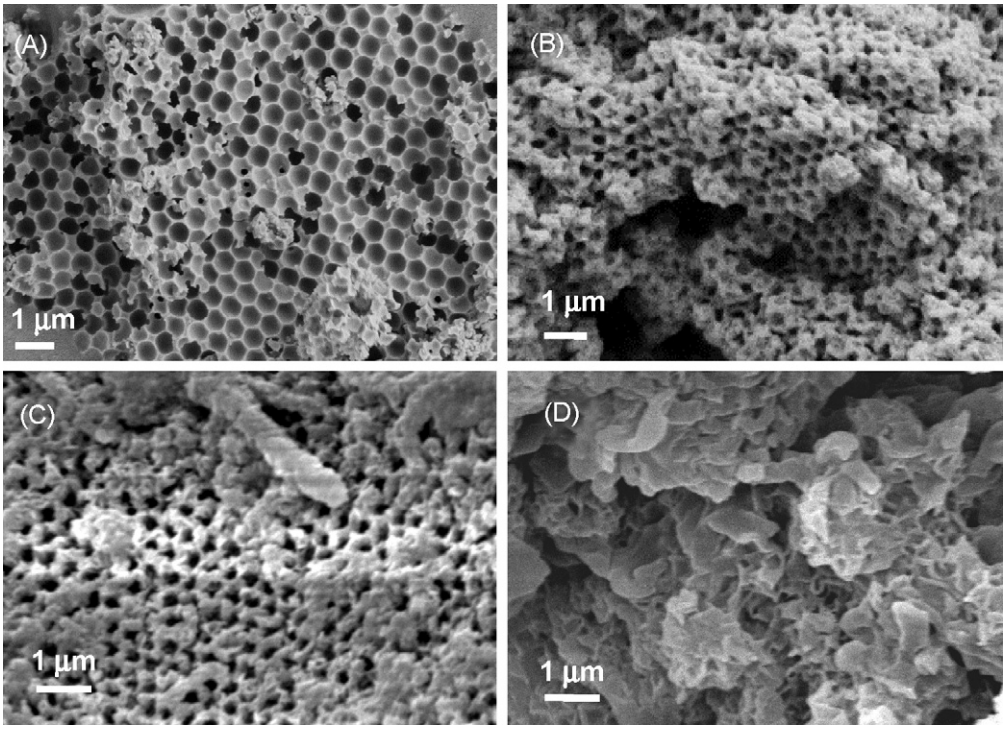

Fig. 4. SEM images of (A) ordered macroporous mixed oxides after calcination process (3DM-MOX), (B) 3DM-MOX regenerated in aqueous solution of DDS, (C) 3DM-MOX regenerated in aqueous solution of iron(III) porphyrin [Fe(TCFSPP)] and (D) intercalated DDS 3DM-LDH exchanged by iron(III) porphyrin [Fe(TCFSPP)/LDH].

of the Soret band associated with a significant amount of free-base porphyrin [39,25], occurred. The Soret peaks of the immobilized phases (Fig. 5b, d, e, g–i) are slightly shifted to higher wavelengths compared to those of the pure FePs [Fig. 5a and c (408 nm) and f (408 nm)]. This behavior can be attributed to steric constraints caused by the support, which substantially distort the FeP molecule in these supported catalysts [57]. Peak broadening is also observed in the case of the intercalated FePs compared with the parent complexes in solution, which can also be explained by the presence of the different intermolecular interactions.

Attempts were done in order to characterize the obtained solids by infrared spectroscopy (diffuse reflectance) but the characteristic bands of the metalloporphyrins were not observed due to the high intensity of the bands of the support (spectra not shown).

Fig. 6 shows the EPR spectra of the solids obtained after the FeP/macro-LDH immobilization process. All the spectra display a common signal in $g = 5.8$ (axial symmetry), typical of a high-spin 5/2 FeP complex [35,41,42,64]. There is also a small distortion from the rhombic symmetry, as seen from the signal in $g = 4.3$, confirming the influence of the support. The higher intensity of the signal due to axial symmetry in $g = 5.8$ suggests that no demetallation occurs during the immobilization procedure [31,35,43], as suggested by the UV–vis data.

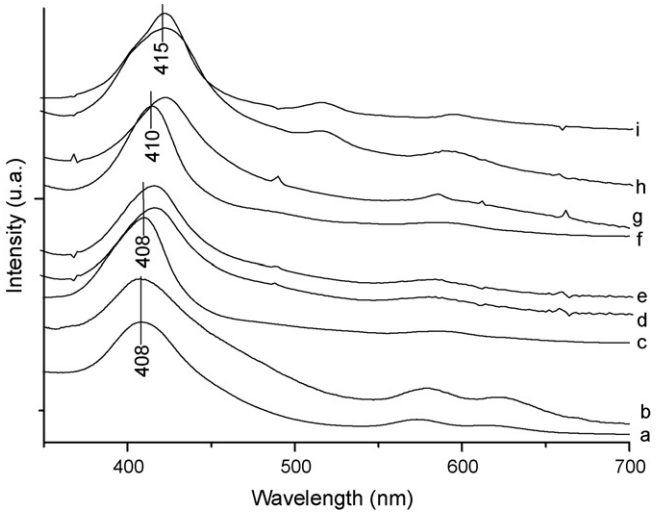

Fig. 5. UV–vis spectra of the FePs and FeP-LDHs in glycerin mull. (a) Fe(TSPP), (b) Fe(TSPP)-LDH, (c) Fe(TDFSPP), (d) Fe(TDFSPP)-LDH, (e) Fe(TDFSPP)-LDH-DDS, (f) Fe(TDCSPP), (g) Fe(TDCSPP)-LDH-DDS, (h) Fe(TCFSPP)-LDH and (i) Fe(TCFSPP)-LDH-DDS.

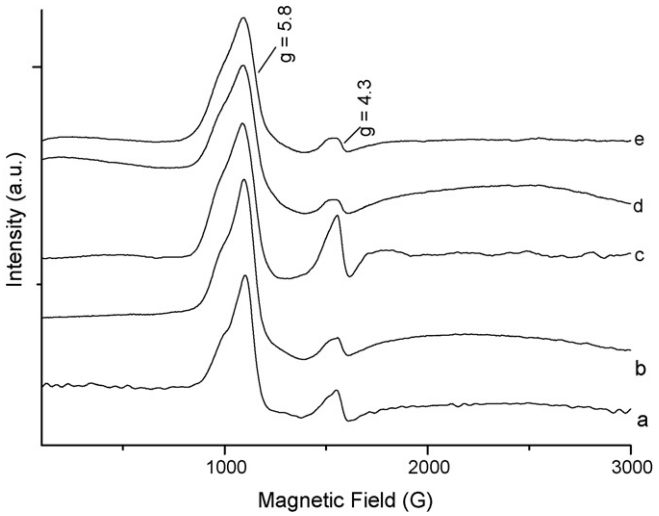

Fig. 6. EPR spectra of solid samples obtained at 77 K. (a) Fe(TDCSPP)-LDH-DDS, (b) Fe(TCFSPP)-LDH-DDS, (c) Fe(TDFSPP)-LDH-DDS, (d) Fe(TDFSPP)-LDH and (e) Fe(TCFSPP)-LDH.

Table 2
Oxidation of cyclooctene by PhIO catalyzed by the homogeneous and immobilized [Fe(TDFSPP)], [Fe(TCFSPP)] and [Fe(TDCSPP)][a].

Catalyst	Run	Cyclooctenoxide[b]
[Fe(TDFSPP)][c]	1	79
[Fe(TDFSPP)]/LDH	2	61
[Fe(TDFSPP)]/LDH-DDS	3	45
[Fe(TCFSPP)][c]	4	28
[Fe(TCFSPP)]/LDH	5	68
[Fe(TCFSPP)]/LDH-DDS	6	58
[Fe(TDCSPP)][c]	7	76
[Fe(TDCSPP)]/LDH	8	40
[Fe(TDCSPP)]/LDH–DDS	9	33
LDH ($Mg_2Al(OH)_6(CO_3)_{0.5}$)[d]	10	6
LDH-DDS[d]	11	9
(PhIO + substrate + solvent)[d]	12	6

[a] Conditions: purged argon, cyclooctene/solvent mixture CH_2Cl_2:CH_3CN 1:1 (v/v) at room temperature. FeP/PhIO/substrate molar ratio = 1:10:1000.
[b] Yields based on starting PhIO obtained after 1 h of reaction.
[c] Homogeneous catalysis was carried out under identical conditions, in dichloromethane/acetonitrile 1:1 solvent mixture (v/v).
[d] Control reactions performed in the same conditions as the oxidation reaction described in (a).

3.2. Investigation of the catalytic activity of the immobilized FePs

C–H bond activation by oxidation under biomimetic conditions makes use of a number of oxygen atom donors, such as iodosylbenzene [10,11,23,35,65], hydrogen peroxide [66], and dioxygen [67,68]. Here we report the use of iodosylbenzene as oxygen donor since metalloporphyrin–PhIO is a classical biomimetic system that can produce the same intermediate catalytic species in the presence of different FePs [11].

The second generation FePs [Fe(TDFSPP)], [Fe(TDCSPP)], and [Fe(TCFSPP)] immobilized into macro-LDH ([Fe(TDFSPP)]-LDH, [Fe(TCFSPP)]-LDH, [Fe(TDCSPP)]-LDH, [Fe(TDFSPP)]-LDH-DDS, [Fe(TCFSPP)]-LDH-DDS, and [Fe(TDCSPP)]-LDH-DDS) were investigated by means of the model reactions cyclooctene epoxidation, cyclohexane hydroxylation, and heptane hydroxylation. The catalytic activity of the first generation [Fe(TSPP)] was not explored here since this iron porphyrin presents low catalytic activity for the oxidation of these substrates [69].

3.2.1. Cyclooctene

It is well known that the oxidation of cyclooctene by metalloporphyrin/PhIO systems produces epoxide as the oxidation product, with no traces of allylic alcohol or ketone [70]. For this reason, cyclooctene is frequently employed as a diagnostic substrate in biomimetic catalytic systems involving metalloporphyrins. In this work we used this alkene to investigate the efficiency and stability of the immobilized anionic FePs as catalysts for alkene oxidation by PhIO. This study also provided information about the accessibility of the substrate and the oxidant to the iron(III) sites in the intercalated catalyst.

The results from cyclooctene epoxidation by PhIO catalyzed by the FePs either in solution (homogeneous catalysis) or immobilized on macro-LDH and macro-LDH-DDS are presented in Table 2, runs 1–9. The results can be divided into two parts: product yields obtained with the FePs [Fe(TDFSPP)] and [Fe(TDCSPP)] and results achieved with [Fe(TCFSPP)].

For both [Fe(TDFSPP)] and [Fe(TDCSPP)], cyclooctenoxide yields obtained in homogeneous medium were better than those achieved with the heterogeneous catalysts, and the catalytic results obtained with FeP-LDH-DDS were lower compared to those achieved with FeP-LDH. This suggests that FePs immobilized into LDH and LDH-DDS provide a more restricted access of the reactants, mainly the bulkier cyclooctene, to the metal center immobilized within the LDH layered structure. The presence of extra DDS anions in the solid LDH-DDS can offer an additional barrier to the mobility of the free reactants toward the catalytic metal center, as evidenced by the lower yields obtained with the FeP-LDH-DDS catalysts.

As for [Fe(TCFSPP)], a better yield is observed in the case of the heterogeneous catalyst [Fe(TCFSPP)]-LDH (Table 2, runs 5 and 6) compared with the homogeneous counterpart (Table 2, run 4). This phenomenon is not easy to explain. It could be due to a better access of the reactants to the metal center of [Fe(TCFSPP)] compared with the other two second generation anionic FePs. This could be caused by the differences in the volume of the substituents in the ortho position of the mesoaryl rings of the various FePs, leading to some distortion of the porphyrin ring as well as differences in the angle formed between the porphyrin plane and the meso substituents [38]. The operation of one of these phenomena or of both could provide ways for the substrate to access the metal center of the [Fe(TCFSPP)] immobilized within the LDH. Similarly to [Fe(TDFSPP)]-LDH-DDS and [Fe(TDCSPP)]-LDH-DDS, the presence of DDS in the [Fe(TCFSPP)]-LDH-DDS solid also lowers the product yield. As explained in the previous paragraph, creation of a specific environment for the catalyst by the extra DDS on the support probably hinders the access of the reactants to the active catalytic species. Alternatively, the explanation could arise from the different location of the FeP molecules located on the surface (reconstructed samples) or in the interlayer (DDS samples).

Control reactions using PhIO in the same reaction conditions (Table 2, runs 10–12), having pristine LDH containing no FeP as catalyst (runs 10–11) and in the absence of FePs and the LDHs phases (run 12), led to lower yields of the oxidation product. This confirms that the catalytic activity observed in runs 1–9 is really due to the FeP complexes.

3.2.2. Cyclohexane

Cyclohexane is a very useful substrate for investigation of the efficiency of FePs as catalysts for alkane hydroxylation by iodosylbenzene (PhIO) [10,23,31,71,72]. The activation of inert C–H bonds in alkanes calls for more drastic conditions than those necessary for alkene functionalization, thus allowing for a better differentiation between the performances of a metalloporphyrin catalyst in solution and immobilized into a solid support.

The results obtained from cyclohexane hydroxylation by PhIO catalyzed by the immobilized FePs studied in this work are presented in Table 3. Both homogeneous and heterogeneous catalyses lead to selective alcohol formation (Table 3), as expected for systems based on FeP catalysts [1,32,35,37,41,58,71]. Neutral FePs containing electron-withdrawing substituents are very efficient and selective for cyclohexane hydroxylation to cyclohexanol, and alcohol yield is directly related to the increase in the electron deficiency of the FeP complex. In fact, [Fe(TDFPP)] hydroxylates cyclohexane at a faster rate and with higher yields than [Fe(TDCPP)] [22]. With the negatively charged electron-withdrawing FeP family used here, the same behavior is observed (Table 3, runs 1, 6 and 11) in homogeneous catalysis. As for heterogeneous catalysis (Table 3, runs 2, 4, 7, 9, 12 and 14), lower yields were observed compared with the reactions carried out in homogeneous medium (runs 1, 6 and 11). As already observed in the case of cyclooctene epoxidation, immobilization of the three anionic FePs into LDH probably leads to a more restricted access of the cyclic substrate to the active intermediate metal-oxo species within the support.

Table 3 (runs 3, 5, 8, 10, 13 and 15) shows that reuse of the heterogeneous catalysts gives similar or higher yields than the first use, suggesting that the catalysts are not released from the surface after their first utilization. The increase in the catalytic yields following the first reaction, after which the solid catalyst was recovered from the reaction medium by filtration, washed, and dried, suggests a

Table 3
Cyclohexane oxidation by PhIO catalyzed by homogeneous and immobilized FePs [Fe(TDFSPP)]; [Fe(TCFSPP)] and [Fe(TDCSPP)][a].

Catalyst	Run	Alcohol % yield[b]
[Fe(TDFSPP)][c]	1	22
[Fe(TDFSPP)]-LDH	2	5
Recycling run[d]	3	19
[Fe(TDFSPP)]-LDH-DDS	4	13
Recycling run[d]	5	37
[Fe(TDCSPP)][b]	6	13
[Fe(TDCSPP)]-LDH	7	6
Recycling run[d]	8	21
[Fe(TDCSPP)]-LDH-DDS	9	7
Recycling run[d]	10	30
[Fe(TCFSPP)][b]	11	10
[Fe(TCFSPP)]-LDH	12	9
Recycling run[d]	13	10
[Fe(TCFSPP)]-LDH-DDS	14	7
Recycling run[d]	15	17
LDH ($Mg_2Al(OH)_6(CO_3)_{0.5}$)[e]	16	Trace
LDH-DDS[e]	17	Trace

[a] Typical conditions: purged argon, catalyst/oxidant/cyclohexane molar ratio = 1 mmol:10 mmol:1000 mmol; solvent mixture dichloromethane/acetonitrile 1:1 (v/v) (350 μL) at room temperature (yields obtained after 1 h of reaction based on starting PhIO). It was assumed that 2 mol of PhIO are necessary for ketone formation.

[b] Total cyclohexanol yields.

[c] Homogeneous catalysis was carried out under identical conditions, in dichloromethane/acetonitrile 1:1 solvent mixture (v/v).

[d] Recycling reactions performed with the same solid catalysts in the same molar ratio and under the same reaction conditions as described in (a).

[e] Control reaction performed with LDH, PhIO and substrate without solid catalyst or FeP in solution carried out under identical conditions as described in (a). All reactions gave only traces of ketone as co-product.

possible reorganization of the FeP anions in the LDH matrix, which should facilitate the access of the reactants to the active catalytic site [8,9]. The best recycling results were obtained with the FePs immobilized into macro-LDH-DDS. This suggests that the presence of DDS in the support makes the first reaction difficult, as observed in the case of cyclooctene, but throughout the process involved in catalyst recovery (especially during catalyst washing), the intercalated DDS anion can be removed from the support. This in turn aids access of the substrate to the metal center and facilitates the catalytic reaction. The analyses of DDS content in the samples after the catalytic reactions were not conducted to confirm the hypothesis.

In the catalytic reactions performed in the absence of the catalyst (Table 3, runs 16 and 17), virtually no products are observed (around 1%). This shows that the obtained yields are really due to the catalytic activity of FePs.

3.2.3. Heptane

Alkane oxidation in the terminal position, to yield alcohols or linear acids, is of great interest for the chemical industry. Linear alkanes are difficult to hydroxylate: the alkane C–H bond is notoriously inert because of its high bond strength, making alkanes ideal solvents for use with very reactive oxidation catalysts. Additionally, the activation energies for subsequent oxidations of an alcohol are similar to the energy required for the initial hydroxylation of the starting alkane, resulting in a mixture of alcohol, ketone/aldehyde, and carboxylic acid products in most alkane oxidation reactions. The similarity of methylene C–H bond strengths in a linear alkane and the lack of functional groups that can serve direct catalysis make the selective hydroxylation of these compounds especially challenging. In general, alkanes have inert C–H bonds and are largely resistant to the oxidation process, mainly in terminal chain positions. The difficulty in promoting terminal oxidation is due to the relative energies associated with C–H bonds (from 101 to 99 to 96 kcal/mol for primary, secondary and tertiary carbon atoms, respectively). Strong oxidants like sulfuric acid, chromic acid, potas-

Table 4
Oxidation of heptane by PhIO catalyzed by homogeneous and immobilized [Fe(TDFSPP)], [Fe(TCFSPP)] and [Fe(TDCSPP)][a].

Catalysts	Run	Time (h)	1-ol (%)[b]	2-ol (%)[c]	3-ol (%)[d]	Total ol (%)[e]	Total one (%)[f]
[Fe(TDFSPP)][g]	1	1	2	3	3	8	<1
	2	24	3	4	3	10	<1
[Fe(TDFSPP)]-LDH	3	1	2	6	5	13	2
	4	24	12	4	4	20	2
[Fe(TDFSPP)]-LDH-DDS	5	1	1	2	2	5	<1
	6	24	5	2	2	9	<1
[Fe(TCFSPP)][g]	7	1	2	3	2	7	–
	8	24	3	3	2	8	<1
[Fe(TCFSPP)]-LDH	9	1	2	4	3	9	2
	10	24	12	3	2	17	2
[Fe(TCFSPP)]-LDH-DDS	11	1	1	3	3	7	<1
	12	24	12	2	2	16	<1
[Fe(TDCSPP)][g]	13	1	3	3	2	8	<1
	14	24	2	2	1	5	<1
[Fe(TDCSPP)]-LDH	15	1	2	2	2	6	3
	16	24	12	2	2	16	2
[Fe(TDCSPP)]-LDH-DDS	17	1	1	2	1	4	<1
	18	24	11	2	1	14	<1

[a] Typical conditions: purged argon, catalyst/oxidant/heptane molar ratio = 1 mmol:10 mmol:1000 mmol; solvent mixture dichloromethane/acetonitrile 1:1 (v/v) (350 μL) at room temperature (yields obtained after 1 h of reaction based on starting PhIO). It was assumed that 2 mol of PhIO are necessary for ketone formation.

[b] Total alcohol (ol) yield (1-heptanol).

[c] Total alcohol (ol) yield (2-heptanol).

[d] Total alcohol (ol) yield (3-heptanol).

[e] Total alcohol yield.

[f] Total ketone (one) yield (4-heptanone). In this work the alcohol in position 4 was not monitored.

[g] Homogeneous catalysis was carried out under identical conditions, in dichloromethane/acetonitrile 1:1 solvent mixture (v/v).

sium permanganate, among others, can perform this reaction, but they are not environmentally acceptable. Consequently, they are not commonly employed. Studies have been made in an attempt to make efficient clean catalysts that are able to promote oxidation reactions in mild conditions, using environmentally acceptable oxidants such as hydrogen peroxide, which generates only H_2O and O_2 after the catalysis [73–80]. Enzymes, metal-complex catalysts, and metal-based biomimetic systems are known to induce regioselective transformations of linear alkanes, but their application is still a hard task [5,81,82]. In this sense, metalloporphyrin systems have been intensively investigated as catalysts for these less reactive substrates [73,83,84] in a biomimetic way.

In the absence of steric constraints, the regioselectivity for C–H bond activation during the hydroxylation of linear alkanes is expected to be determined by the relative bond dissociation energy [72]. A similar statistical product distribution is expected for carbon products at positions 2 and 3, and there is no significant preference for one carbon 2 (or 3) over another carbon 2 (or 3) [84].

The catalytic results obtained for the three anionic FePs studied here, both in solution and immobilized into macro-LDH, in the oxidation of heptane are presented in Table 4.

Although heptane oxidation can lead to different alcohol and ketone products (in the 1, 2, 3 and 4 carbon chain positions), all the catalysts used here promoted good selectivity for alcohols in positions 1, 2 3 and 4. High selectivity for the alcohol products is also observed in biological systems [5].

The catalytic behavior of the three FeP complexes in homogeneous medium (Table 4, runs 1, 7 and 13) is similar to the catalytic performance observed for metalloporphyrins in general. Reactions with metalloporphyrins in homogeneous systems are usually selective for the alcohol in positions 2 or 3, because less energy is necessary for activation of these C–H bonds compared with position 1, for example. Suslick and co-author [84] observed some selectivity for position 1 of hexane when they used metalloporphyrin systems.

With bulky catalysts, because of the structure of the porphyrin [73] in homogeneous catalysis or because of immobilization into the support [38], it is expected that the access of the linear alkane to the metal center should be restricted to the more exposed C–H bond at carbon 1, giving rise to shape-selectivity, as observed by Suslick et al. in homogeneous catalysis. On the other hand, micro- and mesoporous materials containing relatively small cavities or narrow channels are excellent examples of heterogeneous catalysts for the regioselective functionalization of long-chain alkanes [85,86]. It is expected that the immobilization of metallocomplexes into this kind of materials should also promote some regioselectivity in the oxidation of terminal linear alkanes. Using the heterogeneous catalyst resulting from immobilization of the FePs into macro-LDH and LDH-DDS (Table 4), regioselectivity for the hydroxylation of the more sterically accessible methyl groups (carbon 1) was surprisingly observed (Table 4).

The difference in regioselectivity observed from the catalytic results concerning homogeneous and heterogeneous systems suggests that the FeP-LDH assembly can generate a restricted space that is suitable for the approach of the n-alkane in a way that terminal oxidation is favored over secondary carbon oxidation. The influence of the environment provided by the support on substrate access to the catalytic center, as well as on the positioning of the catalyst in the support can be inferred [13]. The macro-LDHs have a differentiated structure that should create a favorable confined chemical environment, thus allowing the keying of the linear alkane molecule into the pore, leading to selective reactions.

Finally, interesting results were obtained for reactions carried out for a period of 24 h. Higher yields were observed for the alcohol in heterogeneous catalysis (Table 4, runs 4, 10, 12, 16, and 18) compared with homogeneous catalysis (Table 4, runs 2, 8, and 14). Furthermore, 24-h led to selectivity toward 1-heptanol, thus suggesting that the longer reaction time favors substrate access to the catalytic active species confined in the structure of the solid support.

4. Conclusions

First and second generation iron(III)porphyrins have been successfully immobilized into macroporous LDH support using both the reconstruction of nanostructured mixed oxides (3DM-MOX) and the anionic exchange methods. Six different solid catalysts were obtained by immobilization of the FePs on/into the macro-LDH, obtained by reconstruction of the nanostructured mixed oxides, templated by polystyrene nanospheres. Compared with the LDH obtained by co-precipitation without a template, metalloporphyrins immobilized on/into macro-LDH exhibited different behavior as catalysts for hydrocarbon oxidation reactions. This behavior can be explained by creation of an active channel on the support, which changes the efficiency and selectivity of the metalloporphyrins in oxidation reactions. All the heterogeneous catalysts were highly stable, and the recyclability of the catalysts was proven for cyclohexane hydroxylation. The most positive effect of the immobilization of the three FePs in macro-LDH was observed in the oxidation of the linear alkane heptane: selectivity for the alcohol product was observed when reaction times of 24 h were used for all the heterogeneous catalysts. Probably, the particular structure of the support with channel and micro-environments can create a suitable structure for the access of the terminal position of the substrate for this family of biomimetic catalysts in the case of the selective oxidation in position C1 of the linear alkane. Increasing the reaction time has a positive effect on reactant diffusion into the metal center, thus improving catalyst performance.

Acknowledgments

The authors acknowledge the financial support of Coordenação de Aperfeiçoamento de Pessoal de Nível Superior (CAPES) and Conselho Nacional de Desenvolvimento Científico e Tecnológico (CNPq), as well as the contribution of Fundação Araucária, Fundação da Universidade Federal do Paraná (FUNPAR), Universidade Federal do Paraná (UFPR), Laboratoire des Matériaux Inorganiques (LMI), Centre National de la Recherche Scientifique (CNRS), and Université Blaise Pascal.

References

[1] D. Mansuy, C. R. Chimie 10 (2007) 392–413.
[2] D. Mansuy, Catal. Today 138 (2008) 2–8.
[3] Y. Cai, Y. Liu, Y. Lu, G. Gao, M. He, Catal. Lett. 124 (2008) 334–339.
[4] A. Agarwala, D. Bandyopadhyay, Catal. Lett. 124 (2008) 392–396.
[5] M.W. Peters, P. Meinhold, A. Glieder, F.H. Arnold, J. Am. Chem. Soc. 125 (2003) 13442–13450.
[6] M. Newcomb, P.H. Toy, Acc. Chem. Res. 33 (2000) 449–455.
[7] B. Meunier, S.P. Visser, S. Shaik, Chem. Rev. 104 (2004) 3947–3980.
[8] P.R. Ortiz de Montellano, Cytochrome P-450, Structure, Mechanism and Biochemistry, Plenum Press, New York/London, 1986, p. 217.
[9] B. Meunier, Chem. Rev. 92 (1992) 1411–1456.
[10] J.T. Groves, T.E. Nemo, R.S. Meyers, J. Am. Chem. Soc. 101 (1979) 1032–1033.
[11] J.T. Groves, J. Inorg. Biochem. 100 (2006) 434–447.
[12] D. Dolphin, T. Traylor, L.Y. Xie, Acc. Chem. Res. 30 (1997) 251–259.
[13] N.A. Stephenson, A.T. Bell, Inorg. Chem. 46 (2007) 2278–2285.
[14] H. Turk, W.T. Ford, J. Org. Chem. 56 (1991) 1253–1260.
[15] Y. Moro-oka, M. Akita, Catal. Today 41 (1998) 327–338.
[16] T. Chen, E. Kang, G. Tan, S. Liu, S. Zheng, K. Yang, S. Tong, C. Fang, F. Xiao, Y. Yan, J. Mol. Catal. A: Chem. 252 (2006) 56–62.
[17] P. Battioni, J.P. Renaud, J.F. Bartoli, M. Reina-Artiles, M. Fort, D. Mansuy, J. Am. Chem. Soc. 110 (1988) 8462–8470.
[18] D.C. Silva, G. DeFreitas-Silva, E. Nascimento, J.S. Rebouças, P.J.S. Barbeira, M.E.D. Carvalho, Y.M. Idemori, J. Inorg. Biochem. 102 (2008) 1932–1941.
[19] J.F. Bartoli, P. Battioni, W.R. De Foor, D. Mansuy, J. Chem. Soc. Chem. Commun. (1994) 23–24.
[20] T.G. Traylor, S. Tsuchiya, Inorg. Chem. 26 (1987) 1338–1339.

[21] M.H. Lim, S.W. Jin, Y.J. Lee, G.-J. Jhon, W. Nam, C. Kim, Bull. Korean Chem. Soc. 22 (2001) 93–96.
[22] Y.M. Goh, W. Nam, Inorg. Chem. 38 (1999) 914–920.
[23] J.T. Groves, R.C. Haushalter, M. Nakamura, T.E. Nemo, B.J. Evans, J. Am. Chem. Soc. 103 (1981) 2884–2886.
[24] F. Bedioui, Coord. Chem. Rev. 144 (1995) 39–68.
[25] S. Nakagaki, A.R. Ramos, F.L. Benedito, P.G. Peralta-Zamora, A.J.G. Zarbin, J. Mol. Catal. A: Chem. 185 (2002) 203–210.
[26] S. Nakagaki, C.R. Xavier, A.J. Wosniak, A.S. Mangrich, F. Wypych, M. Cantão, I. Denicoló, L.T. Kubota, Colloids Surf. A 168 (2000) 261–276.
[27] A.M. Machado, F. Wypych, S.M. Drechsel, S. Nakagaki, J. Colloids Interface Sci. 254 (2002) 158–164.
[28] R. Naik, P. Joshi, R.K. Deshpande, J. Mol. Catal. A: Chem. 238 (2005) 46–50.
[29] S. Nakagaki, F. Wypych, J. Colloids Interface Sci. 315 (2007) 142–157.
[30] S. Nakagaki, F.L. Benedito, F. Wypych, J. Mol. Catal. A: Chem. 217 (2004) 121–131.
[31] L. Barloy, J.P. Lallier, P. Battioni, D. Mansuy, Y. Pitfard, M. Tournoux, J.B. Valim, W. Jones, New J. Chem. 16 (1992) 71–80.
[32] S. Nakagaki, K.A.D.F. Castro, G.S. Machado, M. Halma, S.M. Drechsel, F. Wypych, J. Braz. Chem. Soc. 17 (2006) 1672–1678.
[33] T. Hibino, W. Jones, J. Mater. Chem. 11 (2001) 1321–1323.
[34] G.S. Machado, K.A.D.F. Castro, F. Wypych, S. Nakagaki, J. Mol. Catal. A: Chem. 283 (2008) 99–107.
[35] M. Halma, F. Wypych, S.M. Dreschel, S. Nakagaki, J. Porphyr. Phthalocya. 6 (2002) 502–513.
[36] S. Nakagaki, G.S. Machado, M. Halma, A.A.S. Marangon, K.A.D.F. Castro, N. Mattoso, F. Wypych, J. Catal. 242 (2006) 110–117.
[37] F.L. Benedito, S. Nakagaki, A.A. Saczk, P.G. Peralta-Zamora, M.C.M. Costa, Appl. Catal. A: Gen. 250 (2003) 1–11.
[38] M.A. Matinez-Lorente, P. Battioni, W. Kleemiss, J.F. Bartoli, D. Mansuy, J. Mol. Catal. A: Chem. 113 (1996) 343–353.
[39] S.S. Cady, T.J. Pinnavaia, Inorg. Chem. 17 (1978) 1501–1507.
[40] M. Chibwe, L. Ukrainczyk, S.A. Boyd, T.J. Pinnavaia, J. Mol. Catal. A: Chem. 113 (1996) 249–256.
[41] S. Nakagaki, M. Halma, A. Bail, G.G.C. Arízaga, F. Wypych, J. Colloids Interface Sci. 281 (2005) 417–423.
[42] F. Wypych, A. Bail, M. Halma, S. Nakagaki, J. Catal. 234 (2005) 431–437.
[43] F. Li, L. Zhang, D.G. Evans, C. Forano, X. Duan, Thermochim. Acta 424 (2004) 15–23.
[44] L. Ren, J.-S. Hu, L.-J. Wan, C.-L. Bai, Mat. Res. Bull. 42 (2007) 571–575.
[45] T. Ishikawa, K. Matsumoto, K. Kandori, T. Nakayama, Colloids Surf. A: Physicochem. Eng. Aspects 293 (2007) 135–145.
[46] T. Stanimirova, T. Hibino, Appl. Clay Sci. 31 (2006) 65–75.
[47] A. Khan, D.J. O'Hare, J. Mater. Chem. 12 (2002) 3191–3198.
[48] V. Rives, M.A. Ulibarri, Coord. Chem. Rev. 181 (1999) 61–120.
[49] Z.Y. Qin, Q.Z. Sun, C.G. Zhang, X.J. Wang, W.A. Zhao, Langmuir 19 (2003) 5570–5574.
[50] Z. Tong, T. Shichi, G. Zhang, K. Takagi, Res. Chem. Intermed. 29 (2003) 335–341.
[51] S. Bonnet, C. Forano, A. de Roy, J.P. Besse, P. Maillard, M. Momenteau, Chem. Mater. 8 (1996) 1962–1968.
[52] E. Géraud, S. Rafqah, M. Sarakha, C. Forano, V. Prevot, F. Leroux, Chem. Mater. 20 (2008) 1116–1125.
[53] S. Abello, F. Medina, D. Tichit, J. Perez-Ramirez, Y. Cesteros, P. Salagre, J.E. Sueiras, Chem. Commun. (2005) 1453–1455.
[54] E. Géraud, V. Prévot, F. Leroux, J. Phys. Chem. Solids 67 (2006) 903–908.
[55] J.S. Lyndsey, I.C. Schreiman, H.C. Hsu, P.C. Kearney, A.M. Marguerettaz, J. Org. Chem. 52 (1987) 827–836.
[56] A. Adler, F.R. Longo, J. Am. Chem. Soc. 86 (1964) 3145–3149.
[57] A. Adler, F.R. Longo, F. Kampas, J. Kim, J. Inorg. Nucl. Chem. 32 (1970) 2443–2445.
[58] J.G. Sharefkin, H. Saltzmann, Org. Synth. 43 (1963) 60–62.
[59] H.J. Lucas, E.R. Kennedy, M.W. Forno, Org. Synth. 43 (1963) 483–485.
[60] J.L. Ou, C.P. Chang, Y. Sung, K.L. Ou, C.C. Tseng, H.W. Ling, M.D. Ger, Colloids Surf. A: Phys. Eng. Aspects 305 (2007) 36–41.
[61] H.S. Panda, R. Srivastava, D. Bahadur, Mater. Res. Bull. 43 (2008) 1448–1455.
[62] T. Kameda, M. Saito, Y. Umetsu, J. Alloys Compd. 402 (2005) 46–52.
[63] S.K. Acharya, A.K. Srivastava, Bowmick, Compos. Sci. Technol. 67 (2007) 2807–2816.
[64] J. Krzystek, A. Ozarowski, J. Telser, Coord. Chem. Rev. 250 (2006) 2308–2324.
[65] W. Nam, Y.O. Ryu, W.J. Song, J. Biol. Inorg. Chem. 9 (2004) 654–660.
[66] B.S. Lane, K. Burgess, Chem. Rev. 103 (2003) 2457–2474.
[67] J.E. Lyons, P.E. Ellis Jr., in: R.A. Sheldon (Ed.), Metalloporphyrins in Catalytic Oxidations, Marcel Dekker, New York, 1994, pp. 297–324.
[68] R. Naik, P. Joshi, J.K. Deshpande, J. Mol. Catal. A: Chem. 238 (2005) 46–50.
[69] M. Halma, K.A.D.F. Castro, C. Taviot-Gueho, V. Prévot, C. Forano, F. Wypych, S. Nakagaki, J. Catal. 257 (2008) 233–243.
[70] A.J. Appleton, S. Evans, J.R. Lindsay Smith, J. Chem. Soc., Perkin Trans. 2.3 (1996) 281–285.
[71] Y. Iamamoto, Y.M. Idemori, S. Nakagaki, J. Mol. Catal. A: Chem. 99 (1995) 187–193.
[72] J. Berkowitz, G.B. Ellison, D. Gutman, J. Phys. Chem. 98 (1994) 2744–2765.
[73] J.F. Bartoli, O. Brigaud, P. Battioni, D. Mansuy, J. Chem. Soc. Chem. Commun. (1991) 440–442.
[74] G.B. Shul'pin, T. Sooknoi, V.B. Romakh, G. Suss-Fink, L.S. Shul'pina, Tetrahedron Lett. 47 (2006) 3071–3075.
[75] V. Mirkhani, M. Moghadam, S. Tangestaninejad, B. Bahramian, Monatshefte Fur Chem. 138 (2007) 1303–1308.
[76] V.N. Shetti, M.J. Rani, D. Srinivas, P. Ratnasamy, J. Phys. Chem. B: Lett. 110 (2006) 677–679.
[77] B. Modén, B.Z. Zhan, J. Dakka, J.G. Santiesteban, E. Iglesia, J. Phys. Chem. C 111 (2007) 1402–1411.
[78] G.B. Shul'pin, G. Suss-Fink, J. Chem. Soc., Perkin Trans. 2 (1995) 1459–1463.
[79] V.B. Romakh, B. Therrien, G. Suss-Fink, G.B. Shul'pin, Inorg. Chem. 46 (2007) 3166–3175.
[80] G.B. Shul'pin, A.R. Kudinov, L.S. Shul'pina, E.A. Petrovskaya, J. Org. Chem. 691 (2006) 837–845.
[81] A.E. Shilov, G.B. Shul'pin, Activation and Catalytic Reactions of Saturated Hydrocarbons in the Presence of Metal Complexes, Kluwer Academic, Dordrecht/Boston/London, 2000.
[82] M.C. Feiters, A.E. Rowan, R.J.M. Nolte, Chem. Soc. Rev. 29 (2000) 375–384.
[83] J.M. Thomas, R. Raja, G. Sankar, R.G. Bell, Acc. Chem. Res. 34 (2001) 191–200.
[84] B.R. Cook, T.S. Suslick, J. Am. Chem. Soc. 108 (1986) 7281–7286.
[85] J.M. Thomas, R. Raja, Chem. Commun. (2001) 675–687.
[86] K.S. Suslick, P. Bhyrappa, J.-H. Chou, M.E. Kosal, S. Nakagaki, D.W. Smithenry, S.R. Wilson, Acc. Chem. Res. 38 (2005) 283–291.